A TRILINEAR THREE-BODY PROBLEM

G. LODGE
171 East Lorain St., Oberlin, OH 44074, USA

J. A. WALSH
Department of Mathematics, Oberlin College, Oberlin, OH 44074, USA

M. KRAMER
Applied Science and Technology Department,
University of California at Berkeley, Berkeley, CA 94720, USA

In this paper we present a simplified model of a three-body problem. Place three parallel lines in the plane. Place one mass on each of the lines and let their positions evolve according to Newton's inverse square law of gravitation. We prove the KAM theory applies to our model and simulations are presented. We argue that this model provides an ideal, accessible entry point into the beautiful mathematics involved in the study of the three-body problem.

Keywords: Three-body; KAM theory; Poincaré map.

1. Introduction

The renowned N-body problem concerns the behavior of N point masses whose motion in three-dimensional space is governed by Newton's inverse square law of gravitation. In solving the two-body problem, Newton explained Kepler's three empirical laws regarding the motion of a planet around the sun [Newton, 1687]. Turning his attention to the three-body problem consisting of the sun, earth and moon, Newton encountered difficulties to the extent that he was prompted to remark "...his head never ached but with the study of the moon" [Westfall, 1980].

Henri Poincaré is arguably the first mathematician to unearth chaotic behavior in a dynamical system. He accomplished this within the context of the (circular planar) restricted three-body problem [Poincaré, 1890]. In this simplified problem, three masses move in a single plane. The two larger masses move in circles about their center of gravity with uniform speed. The third body has "infinitely small" mass, and it is the motion of this small body under the gravitational influence of the two larger bodies that is of interest. Poincaré offered by way of example the sun, Jupiter, and a second, smaller planet perturbed by Jupiter (neglecting the eccentricity of Jupiter and the inclination of the orbits [Barrow-Green, 1997]). Motivated by the restricted three-body problem, Poincaré discovered the existence of transverse homoclinic orbits, yielding chaotic behavior as described below.

The model introduced here is a simple one. It serves to reduce the dimension of the three-body problem by restricting the motion of each mass to a line. It also removes the potential for double and triple collisions occurring in the collinear three-body problem [Kaplan, 1999; McGehee, 1971; Meyer & Wang, 1995] by placing the masses on separate, parallel lines. We believe this model provides an ideal, accessible entry point for those interested in the mathematics of the problem whose study ultimately lead to the creation of nonlinear dynamical systems as a vibrant discipline.

2. Model Equations

Place three parallel lines in the plane, with the top and bottom lines each a distance $\varepsilon/2$ from the center line. Place one body on each line as indicated in Fig. 1. Let m_i and $x_i = x_i(t)$ denote the mass and position, respectively, of body i, $i = 1, 2, 3$, with x_i measured from a fixed vertical axis. Let the masses evolve under Newton's law of gravitation, assuming there is no friction (think of beads on a greased wire). Newton's second law yields the equations of motion

$$\ddot{x}_1 = \frac{m_2(x_2 - x_1)}{((x_2 - x_1)^2 + \varepsilon^2)^{3/2}}$$
$$+ \frac{m_3(x_3 - x_1)}{((x_3 - x_1)^2 + \varepsilon^2/4)^{3/2}}$$
$$\ddot{x}_2 = \frac{m_1(x_1 - x_2)}{((x_1 - x_2)^2 + \varepsilon^2)^{3/2}}$$
$$+ \frac{m_3(x_3 - x_2)}{((x_3 - x_2)^2 + \varepsilon^2/4)^{3/2}} \quad (1)$$
$$\ddot{x}_3 = \frac{m_1(x_1 - x_3)}{((x_1 - x_3)^2 + \varepsilon^2/4)^{3/2}}$$
$$+ \frac{m_2(x_2 - x_3)}{((x_2 - x_3)^2 + \varepsilon^2/4)^{3/2}} \, .$$

We have set the universal gravitational constant G to be unity in the above equations. This can be accomplished, for example, by changing the unit of mass [Meyer & Hall, 1992]. Also note that, due to the introduction of the parameter ε, the vector field in system (1) is smooth.

3. Simplifying Assumptions

Solutions to system (1) lie in $\mathbf{R}^6$. We will reduce the dimension to two via the following standard simplifications. First note that

$$\sum_{i=1}^{3} m_i \ddot{x}_i = 0 \, . \quad (2)$$

Integrating Eq. (2) twice with respect to time yields

$$\sum_{i=1}^{3} m_i x_i = c_1 t + c_2 \quad (3)$$

for some constants c_1 and c_2. Letting $M = m_1 + m_2 + m_3$ and noting $(1/M) \sum_{i=1}^{3} m_i x_i$ is the (x-coordinate of the) center of mass, the motion of the center of mass is linear, i.e. it has zero acceleration for all time. If we introduce coordinates which measure the position of each body relative to the center
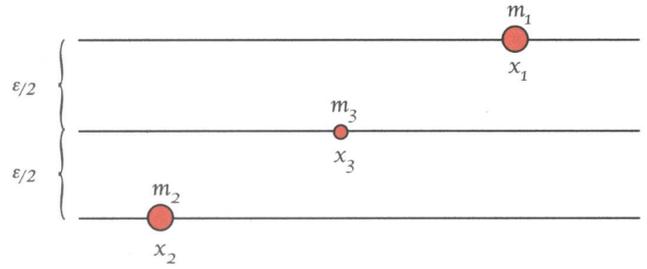

Fig. 1.   The trilinear three-body model.

of mass, the equations of motion do not change. We thus fix the center of mass at the origin by assuming

$$\sum_{i=1}^{3} m_i x_i = 0 \, . \quad (4)$$

Our model is a restricted problem — we assume the center body has negligible mass. This means the center body does not influence the motion of the two larger bodies, though its motion is determined by that of masses m_1 and m_2. We thus set $m_3 = 0$ in system (1). Equation (4) then implies $m_1 x_1 + m_2 x_2 = 0$. Simplifying further, we assume $m_1 = m_2 = m$, yielding $x_2 = -x_1$ and $\dot{x}_2 = -\dot{x}_1$. The positions and velocities of the two large bodies are then symmetric about the origin for all time. Substituting into system (1), we reduce to the four-dimensional system

$$\ddot{x}_1 = -\frac{2m x_1}{(4x_1^2 + \varepsilon^2)^{3/2}}$$
$$\ddot{x}_3 = \frac{m(x_1 - x_3)}{((x_1 - x_3)^2 + \varepsilon^2/4)^{3/2}} \quad (5)$$
$$- \frac{m(x_1 + x_3)}{((x_1 + x_3)^2 + \varepsilon^2/4)^{3/2}} \, .$$

Letting $y_i = \dot{x}_i$, $i = 1, 3$, we have the four first-order equations

$$\dot{x}_1 = y_1$$
$$\dot{y}_1 = -\frac{2m x_1}{(4x_1^2 + \varepsilon^2)^{3/2}}$$
$$\dot{x}_3 = y_3$$
$$\dot{y}_3 = \frac{m(x_1 - x_3)}{((x_1 - x_3)^2 + \varepsilon^2/4)^{3/2}} - \frac{m(x_1 + x_3)}{((x_1 + x_3)^2 + \varepsilon^2/4)^{3/2}} \, .$$
$$(6)$$

4. Further Reductions

As a consequence of our assumption regarding the mass of the center body, the first two equations in system (6) depend on neither x_3 nor y_3. Moreover, the subsystem

$$\dot{x}_1 = y_1$$
$$\dot{y}_1 = -\frac{2mx_1}{(4x_1^2 + \varepsilon^2)^{3/2}} \tag{7}$$

is integrable. The function

$$H(x_1, y_1) = \frac{1}{2} y_1^2 - \frac{1}{2} m \frac{1}{(4x_1^2 + \varepsilon^2)^{1/2}}$$

satisfies $(dH/dt)(x_1(t), y_1(t)) = 0$ for solutions $(x_1(t), y_1(t))$ of system (7). Thus level sets $H(x_1, y_1) = C$ of H correspond to solution curves of (7) and, given x_1, y_1 is subsequently determined (see Fig. 2). This reduces our problem to a three-dimensional system with variables x_1, x_3 and y_3.

We choose initial conditions for the large mass so that its motion is periodic. That is, we assume $x_1(t + \tau) = x_1(t)$, where $\tau = \tau(x_1(0), y_1(0))$ is a function of the initial conditions for the large mass. In particular, any solution to (7) with initial condition $(x_1(0), 0)$ is periodic. (If provided with sufficient initial velocity, the large mass tends to ∞.) In spirit we are following Poincaré's lead in assuming periodic motion for the large masses.

Note that $(x_1, y_1) = (0, 0)$ is an equilibrium solution for (7). Hence, if we set the large mass at rest at the origin, the latter two equations in (6) become

$$\dot{x}_3 = y_3$$
$$\dot{y}_3 = -\frac{2mx_3}{(x_3^2 + \varepsilon^2/4)^{3/2}} . \tag{8}$$

The (x_3, y_3)-phase plane for (8) is similar to that sketched in Fig. 2. In particular, system (8) yields a periodic solution for any initial condition with $y_3(0) = 0$. If we start the large mass within a neighborhood of the origin $(x_1, y_1) = (0, 0)$, we can treat system (6) as a small perturbation of system (8). Our model can then be viewed as a periodically forced nonlinear oscillator: to understand solutions to system (6), we seek to understand solutions to the nonautonomous system

$$\dot{x}_3 = y_3$$
$$\dot{y}_3 = \frac{m(x_1(t) - x_3)}{((x_1(t) - x_3)^2 + \varepsilon^2/4)^{3/2}}$$
$$- \frac{m(x_1(t) + x_3)}{((x_1(t) + x_3)^2 + \varepsilon^2/4)^{3/2}} , \tag{9}$$

where $x_1(t)$ is a (periodic) solution of (7).

5. The Poincaré Map

To obtain our final reduction, we turn to the Poincaré map, introduced in [Poincaré, 1881]. Recalling that $x_1(t)$ is periodic with period τ, we create a planar map by setting the large mass in motion and computing the position and velocity of
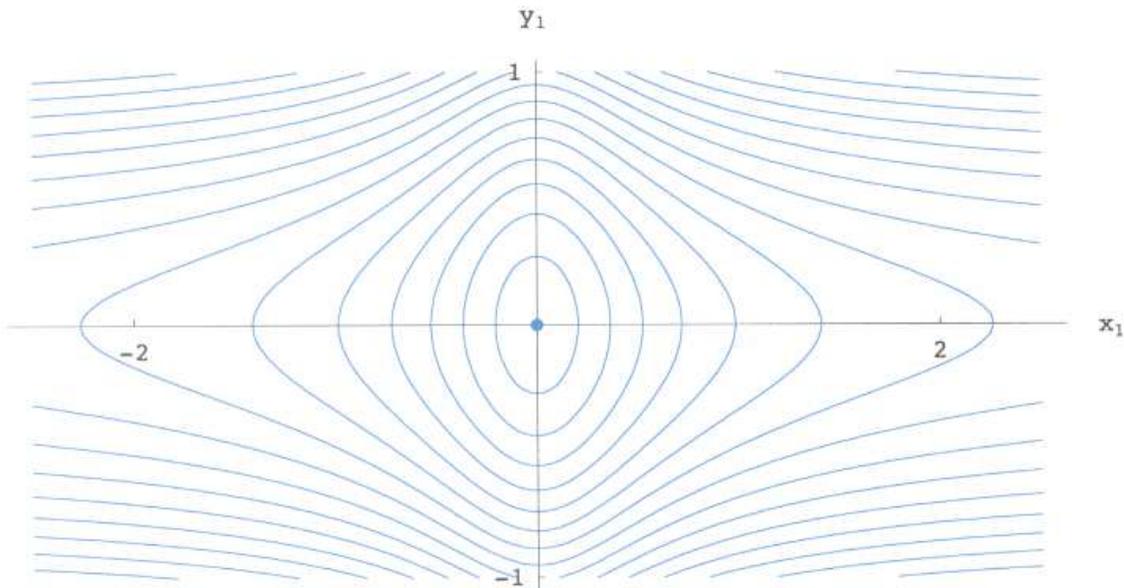

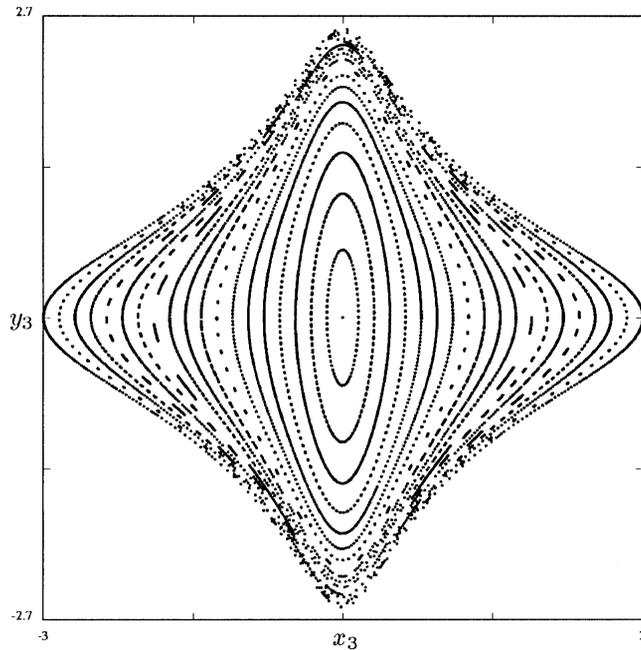Fig. 2.   The (x_1, y_1)-phase plane. The periodic solutions are moving clockwise.

Fig. 3.   A Poincaré map $P : \mathbf{R}^2 \to \mathbf{R}^2$.

Fig. 4.   The rotation number for P as a function of distance from the origin.

the small mass each time the large mass returns to its initial state. This yields the Poincaré map $P_\tau : \mathbf{R}^2 \to \mathbf{R}^2$, $(x_3(0), y_3(0)) \mapsto (x_3(\tau), y_3(\tau))$. The nth iterate of P_τ is then $P_\tau^n(x_3(0), y_3(0)) = (x_3(n\tau), y_3(n\tau))$. A fixed point for P_τ, for example, corresponds to a periodic solution for system (9). We note that P_τ is a diffeomorphism [Perko, 1991].

We let $P : \mathbf{R}^2 \to \mathbf{R}^2$ denote a Poincaré map corresponding to system (8). In this case $x_1(t) = 0$ for all t, so we can sample solutions to (8) at integer multiples of T for any $T > 0$. Several P-orbits for such a Poincaré map are shown in Fig. 3.

The Poincaré map P preserves area for any $T > 0$. This follows from the fact the vector field corresponding to system (8) has zero divergence. Liouville's Theorem then implies the two-dimensional flow corresponding to (8) preserves area. As P is the time-T map for this flow, P must preserve area. We will make use of this observation in Sec. 6.

Let $T > 0$ and let s be the period of a periodic solution Γ for system (8). If s and T are commensurate, every point on Γ is periodic with the same period under the Poincaré map P. If s and T are incommensurate, every point of Γ has a P-orbit which is dense in Γ [Arnol'd & Avez, 1988]. This behavior is evident in Fig. 3.

Corresponding to each periodic solution of (8) is a rotation number [Robinson, 1994], which pro-
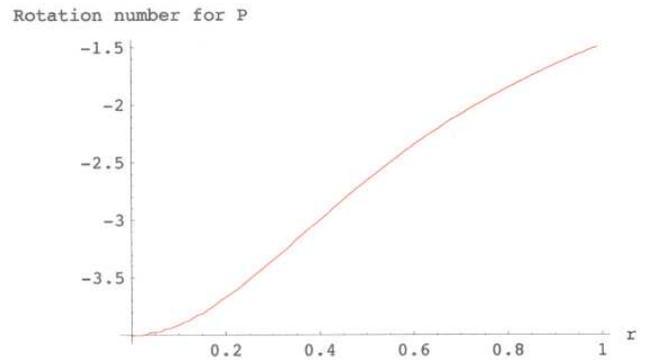
vides a measure of the average counterclockwise "rotation" per iterate of P. The rotation number is rational on curves Γ for which s and T are commensurate, and irrational otherwise. Figure 4 presents a plot of the rotation number for the Poincaré map for system (8) as a function of the distance r from $(x_3, y_3) = (0, 0)$. The rotation numbers are negative because periodic motion in the (x_3, y_3)-phase plane is clockwise. The function is monotonic as the period of a periodic solution to (8) increases with r. For this plot, $\varepsilon = m = T = 1$.

Returning to system (9), we will see that the Poincaré map P_τ is an area-preserving perturbation of P. This will allow us to invoke the KAM/Twist Theorem as the key tool in our analysis.

6.   The Twist Theorem

The celebrated KAM Theorem originated in the work of Kolmogorov [1957] and was proved by Arnol'd [1963] for Poincaré maps of analytic Hamiltonian systems having an arbitrary number of degrees of freedom. An independent proof for planar, area-preserving maps, assuming only sufficient differentiability, was provided by Moser [1962] (also see [Siegel & Moser, 1971]). This latter result is known as Moser's Twist Theorem, and it is this version of the KAM Theorem we refer to here.

The Twist Theorem concerns the existence of invariant simple closed curves for an area-preserving perturbation of an area-preserving mapping of the plane. Recall the P-invariant curves shown in Fig. 3, each with a corresponding rotation number. Any two such curves Γ_1 and Γ_2 bound an annular region. Since the rotation number is a monotonic function of the distance from $(x_3, y_3) = (0, 0)$, points rotate a decreasing amount per iterate of P when moving

from the inner boundary Γ_1 to Γ_2. This provides the "twist" action referred to above.

The Twist Theorem states that if the rotation number on a P-invariant curve is sufficiently irrational and the perturbation is sufficiently small, there exists an invariant simple closed curve for the perturbed map on which all orbits are dense. If the perturbed map is the Poincaré map of a three-dimensional flow, these invariant curves give rise to invariant tori in 3-space. Perturbed solutions either lie on one of these tori, or are trapped between pairs of such tori, and hence are stable in the sense that they are confined to a bounded region in phase space.

In the following statement of the Twist Theorem [Hale & Koçak, 1991], mapping (10) is an area-preserving perturbation of an area-preserving twist map $(r, \theta) \mapsto (r, \theta + \gamma(r))$ defined on the annulus $a \leq r \leq b$. The rotation number for the unperturbed map on a circle of radius $r = r_0$ is $\gamma(r_0)$, and the assumption $\gamma'(r) \neq 0$ ensures this is a twist map. The function $\mathbf{g}$ is 2π-periodic in θ.

Finally, the Twist Theorem is stated for mappings of an annulus due to the introduction of action-angle coordinates for systems such as (6). In these "nonlinear polar coordinates" the simple closed curves in Fig. 3 are circles [Guckenheimer & Holmes, 1983].

Twist Theorem. *Consider in polar coordinates the following area-preserving perturbation of a twist map*

$$\begin{pmatrix} r \\ \theta \end{pmatrix} \mapsto \begin{pmatrix} r \\ \theta + \gamma(r) \end{pmatrix} + \delta \mathbf{g}(\delta, r, \theta) \qquad (10)$$

defined in an annulus $a \leq r \leq b$ such that $d\gamma/dr \neq 0$, the function $\mathbf{g}$ is C^5, and $|\delta|$ is sufficiently small. Then, given any number ω between $\gamma(a)$ and $\gamma(b)$ incommensurable with 2π, and satisfying

$$\left| \frac{\omega}{2\pi} - \frac{p}{q} \right| \geq c|q|^{-5/2}$$

for all integers p and q, there exists a differentiable closed curve Γ, which is invariant under the map (10). The orbits on Γ are given by rotation through the angle ω.

Such numbers ω are called Diophantine (or "sufficiently irrational"). Note that the Twist Theorem implies the existence of infinitely many invariant curves for the perturbed map. In fact, Moser's proof shows that the Lebesgue measure of the set of

invariant curves is positive and approaches the measure of the annulus as $\delta \to 0$. References [Arnol'd & Avez, 1988; Arrowsmith & Place, 1990; Barrow-Green, 1997; Guckenheimer & Holmes, 1983; Hale & Koçak, 1991; Hénon, 1983; Katok & Hasselblatt, 1995; Meyer & Hall, 1992; Siegel & Moser, 1971] provide introductions to the KAM theory at various levels.

7. Homoclinic Orbits and Island Chains

Recall the Poincaré map $P : \mathbf{R}^2 \to \mathbf{R}^2$ for system (8). The origin $(0, 0)$ is an elliptic fixed point and sits in a neighborhood containing a continuous family of P-invariant simple closed curves. On these curves the rotation number is a negative, increasing function of distance from the origin. Points nearer $(0, 0)$ thus rotate a greater clockwise angle per iterate of P (see Fig. 5, after [Guckenheimer & Holmes, 1983]).

There is a natural T-value at which to sample solutions to system (8). Linearizing system (7) at the equilibrium point $(x_1, y_1) = (0, 0)$ yields the system of equations

$$\begin{bmatrix} \dot{x}_1 \\ \dot{y}_1 \end{bmatrix} = \begin{bmatrix} 0 & 1 \\ -2m/\varepsilon^3 & 0 \end{bmatrix} \begin{bmatrix} x_1 \\ y_1 \end{bmatrix},$$

corresponding to simple harmonic motion with frequency $\alpha = \sqrt{2m/\varepsilon^3}$. As $(x_1(0), y_1(0)) \to (0, 0)$, the period of the large mass oscillation approaches $2\pi/\alpha$. We set $T = 2\pi/\alpha$ and use this T-value in all that follows.

Chaos arises in our model as follows. Let Γ_1, Γ_2 be P-invariant curves having sufficiently irrational rotation numbers $\omega_1 < \omega_2 < 0$. Let Γ_3 denote a curve between Γ_1 and Γ_2 having rational rotation number $m/n \in (\omega_1, \omega_2)$. Note that every point on Γ_3 is fixed by P^n and rotates through the angle $2\pi m$ every n iterations. Moreover, points on Γ_1 and Γ_2 rotate through angles respectively greater than and less than $2\pi m$ in magnitude every n iterates of P.

Consider the Poincaré map $P_\tau : \mathbf{R}^2 \to \mathbf{R}^2$ introduced in Sec. 5. If the perturbation is small enough (i.e. if the large mass is set in motion in a sufficiently small neighborhood of $(x_1, y_1) = (0, 0)$) and the map P_τ preserves area, then by the Twist Theorem there exist P_τ-invariant closed curves Γ_1', Γ_2' with rotation numbers ω_1 and ω_2, respectively. Points on Γ_1' will still rotate through an angle greater than $2\pi m$ in magnitude (assuming the perturbation is small enough), while those on Γ_2' rotate
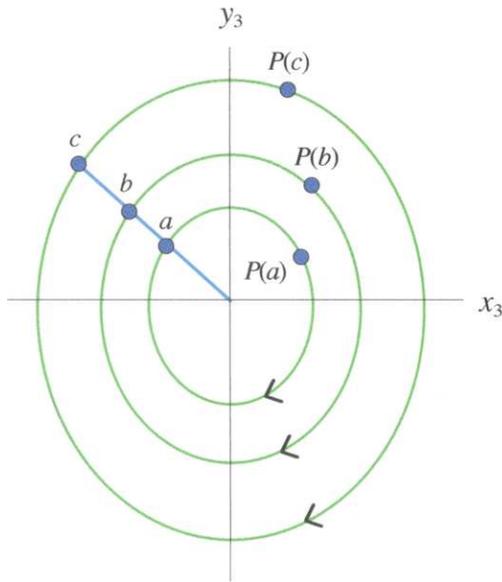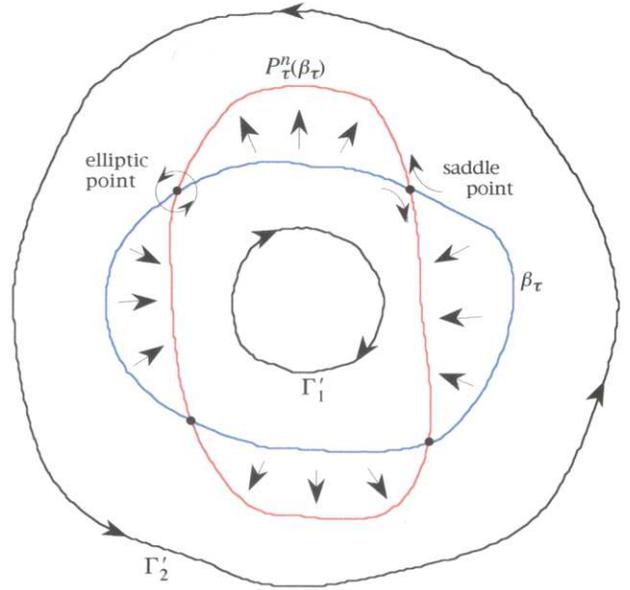
Fig. 5.   Rotation under the Poincaré map P.

Fig. 6.   The curve β_τ and its image under P_τ^n.

through an angle less than $2\pi m$ in magnitude, every n iterations of P_τ. Thus, given a ray $\mathcal{R}$ extending from $(x_3, y_3) = (0, 0)$, there exists a point on $\mathcal{R}$ which rotates precisely $2\pi m$ after n iterations, returning to $\mathcal{R}$. The collection of such points as $\mathcal{R}$ varies is a closed curve which we denote as β_τ.

Assuming P_τ is area-preserving, β_τ and $P_\tau^n(\beta_\tau)$ enclose the same area and therefore must intersect. By the construction of β_τ, each intersection point is a fixed point of P_τ^n. Generically these intersections are transverse, in which case these fixed points are alternately of elliptic and saddle types (see Fig. 6).

Let $W^s(\mathbf{p})$ and $W^u(\mathbf{p})$ denote the stable and unstable manifolds, respectively, of a saddle fixed point $\mathbf{p}$ for a diffeomorphism $F : \mathbf{R}^2 \to \mathbf{R}^2$. Poincaré termed a point $\mathbf{q}$ in the intersection of $W^s(\mathbf{p})$ and $W^u(\mathbf{p})$ a homoclinic point — it is "doubly asymptotic" [Poincaré, 1899] in that $F^n(\mathbf{q}) \to \mathbf{p}$ and $F^{-n}(\mathbf{q}) \to \mathbf{p}$ as $n \to \infty$. A homoclinic orbit provides the stretching and folding behavior indicative of a chaotic dynamical system. Homoclininc points also arise in intersections of stable and unstable manifolds in saddle "loops" as in Fig. 7.

A transverse intersection of $W^s(\mathbf{p})$ and $W^u(\mathbf{p})$ leads to homoclinic tangles and chaotic dynamics, as in the following Smale–Birkhoff Theorem ([Perko, 1991]; also see [Smale, 1965; Guckenheimer & Holmes, 1983; Robinson, 1994]).

Theorem.   *Let $F : \mathbf{R}^2 \to \mathbf{R}^2$ be a diffeomorphism with a saddle fixed point $\mathbf{p}$ for which the stable and unstable manifolds intersect transversally. Then there is an $n > 0$ such that F^n has an invariant cantor set containing*

(i)   *a countable set of periodic orbits of F^n of arbitrarily long periods*

(ii) *an uncountable set of bounded nonperiodic orbits, and*

(iii) *a dense orbit.*

Returning to our model, note that the stable and unstable manifolds of each of the fixed points for P_τ^n lie within the annular region bounded by Γ_1' and Γ_2'. As P_τ preserves area, these manifolds will intersect [Guckenheimer & Holmes, 1983], and generically these intersections are transverse [Arrowsmith & Place, 1990]. We thus expect to see chaotic behavior within the region bounded by Γ_1' and Γ_2'.

The dynamics of the map P_τ are strikingly complex. As there are infinitely many sufficiently irrational rotation numbers on the P-invariant curves in Fig. 3, there are infinitely many annular regions containing homoclinic tangles for P_τ. Moreover, this complexity is repeated in a neighborhood of each of the elliptic fixed points for P_τ^n (for appropriate n) in Fig. 6, leading to a sequence of "island chains" on ever smaller scales ([Arrowsmith & Place, 1990], and Figs. 13–16, 18 and 19).
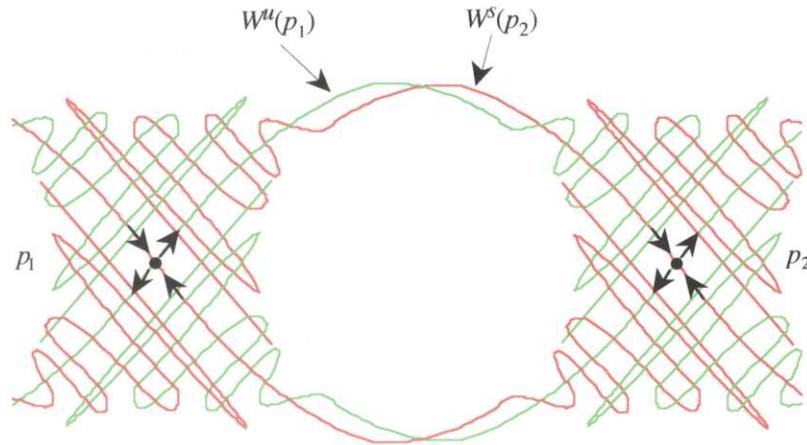
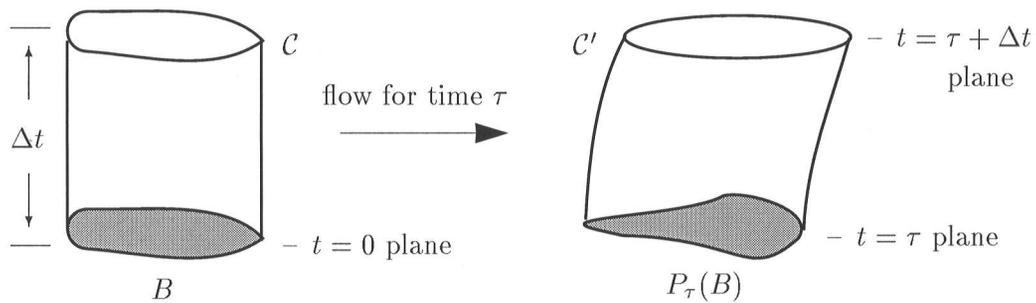Fig. 7.   Transverse crossing of stable and unstable manifolds.

Fig. 8.

The fact P_τ is area-preserving is crucial in the above analysis. Before presenting the model simulations, we prove this fact.

Proposition.   *The map* $P_\tau : \mathbf{R}^2 \to \mathbf{R}^2$ *is area-preserving for all* $\tau > 0$.

Proof.   Convert system (9) to the autonomous system

$$\frac{dx_3}{ds} = y_3$$

$$\frac{dy_3}{ds} = \frac{m(x_1(t) - x_3)}{((x_1(t) - x_3)^2 + \varepsilon^2/4)^{3/2}}$$
$$- \frac{m(x_1(t) + x_3)}{((x_1(t) + x_3)^2 + \varepsilon^2/4)^{3/2}}$$

$$\frac{dt}{ds} = 1 .$$

(11)

Let $\tau > 0$ and $\Delta t > 0$ be given. Let B denote a region in the plane, let $\mathcal{C}$ be the solid with base B and height Δt, and let $\mathcal{C}'$ be the time-τ image of $\mathcal{C}$ under the flow corresponding to system (11) (see Fig. 8). By Liouville's Theorem this flow preserves volume in (x_3, y_3, t)-space. Hence, $\mathrm{Vol}(\mathcal{C}') = \mathrm{Vol}(\mathcal{C}) = \mathrm{Area}(B) \cdot \Delta t$.

For $0 \le u \le \Delta t$, let $A(u)$ denote the area of the intersection of $\mathcal{C}'$ with the $t = u + \tau$ plane. By the Fundamental Theorem of Calculus,

$$\mathrm{Area}(P_\tau(B)) = A(0)$$

$$= \lim_{\Delta t \to 0} \frac{\displaystyle\int_0^{\Delta t} A(u)\,du}{\Delta t}$$

$$= \lim_{\Delta t \to 0} \frac{\mathrm{Vol}(\mathcal{C}')}{\Delta t}$$

$$= \mathrm{Area}(B) . \qquad \blacksquare$$

8. Model Dynamics

We present model simulations in the following sequence of plots. Each figure contains several P_τ-orbits in the (x_3, y_3)-plane. Recalling that τ, the period of the large mass oscillation, depends on the initial condition $(x_1(0), 0)$, we treat $A = x_1(0)$ as the parameter and investigate model behavior as A is varied. For $A \ll 1$, P_τ is a small perturbation of
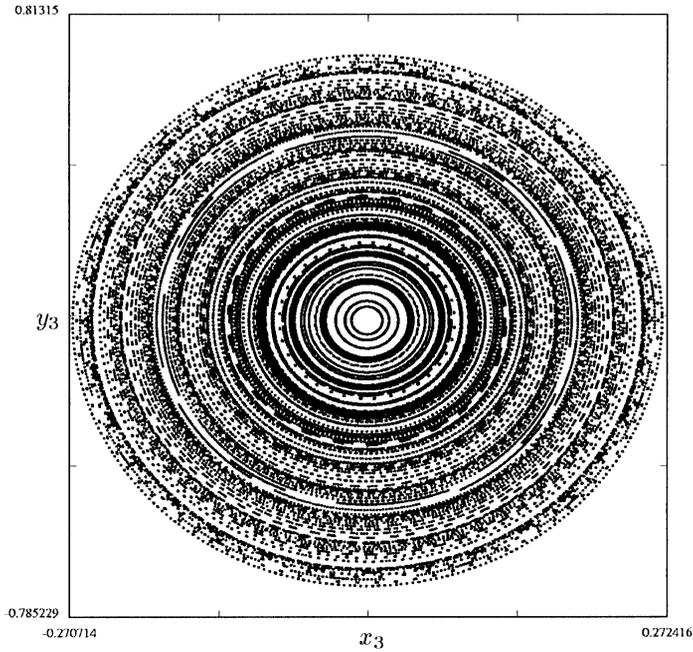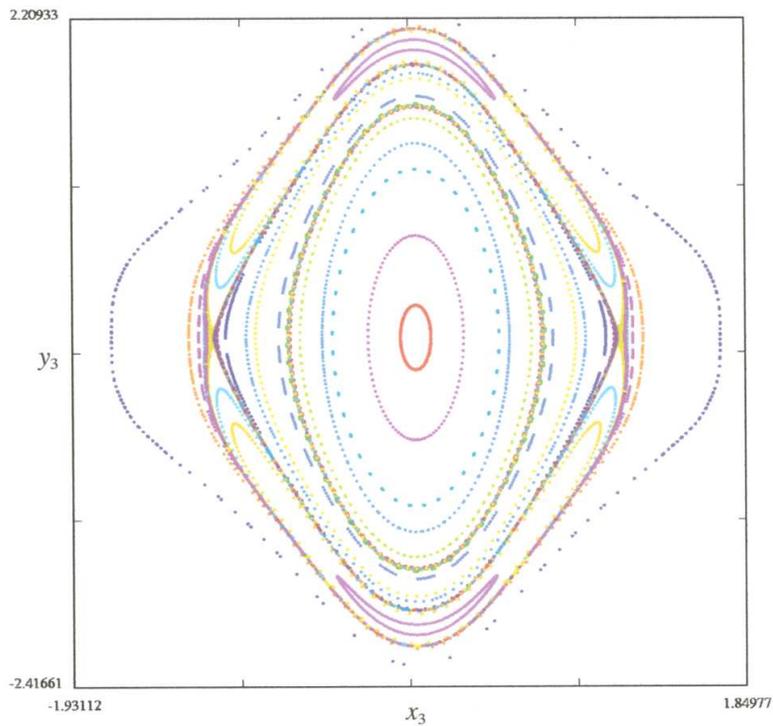

Fig. 9. $A = 0.2$.

Fig. 10.   A larger neighborhood of the origin, $A = 0.2$.

the Poincaré map P and the Twist Theorem provides insight into the behavior of m_3 and the persistence of invariant curves.

Each of Figs. 9–16, 18 and 19 was generated using the software *dstool* [Back *et al.*, 1992] with $\varepsilon = m = 1$. In Figs. 11–13, 15 and 16, P_τ was iterated the same number of times using the same set of initial conditions evenly spaced along the negative x_3-axis. We present one-half of the (x_3, y_3)-plane due to the symmetry of our system. We also
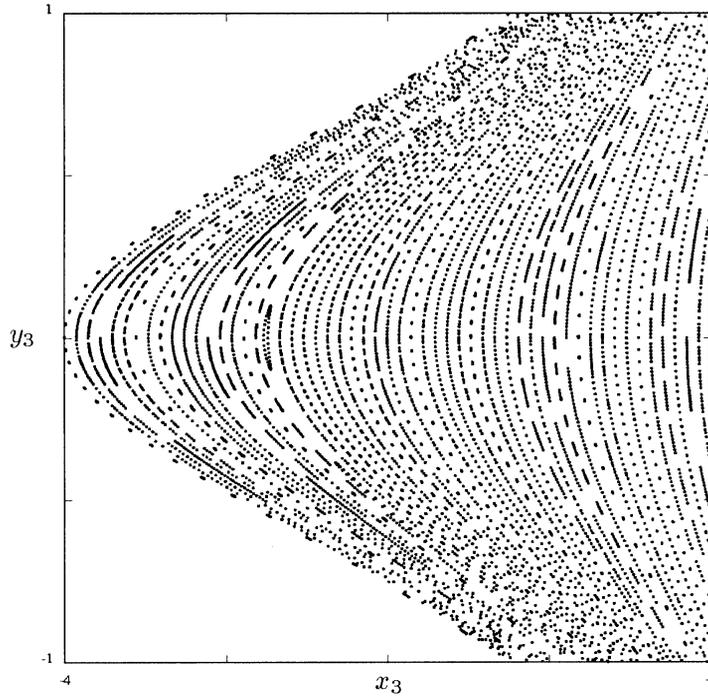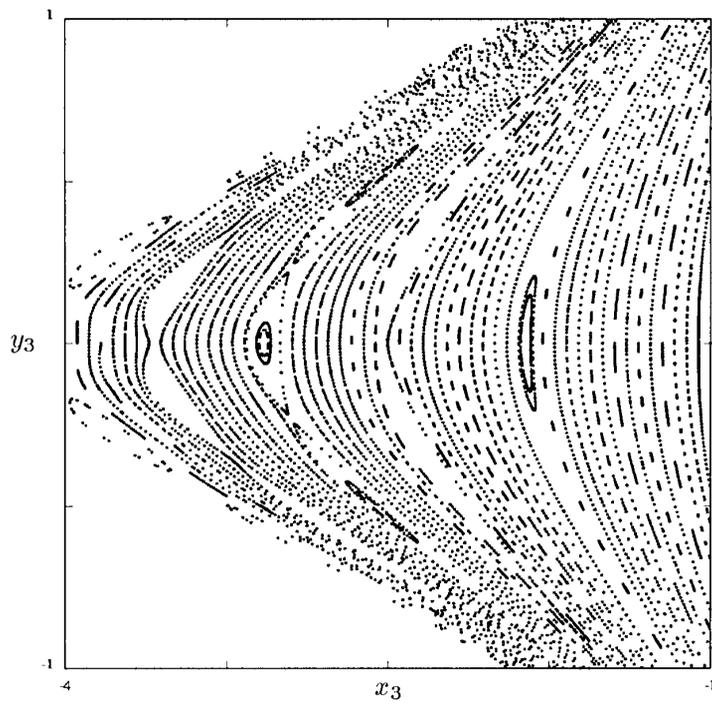

Fig. 11. $A = 0.01$.
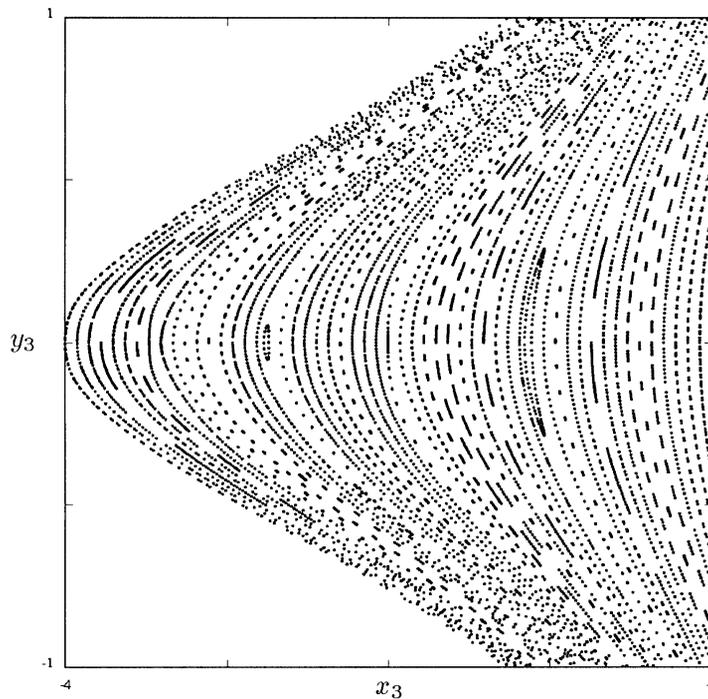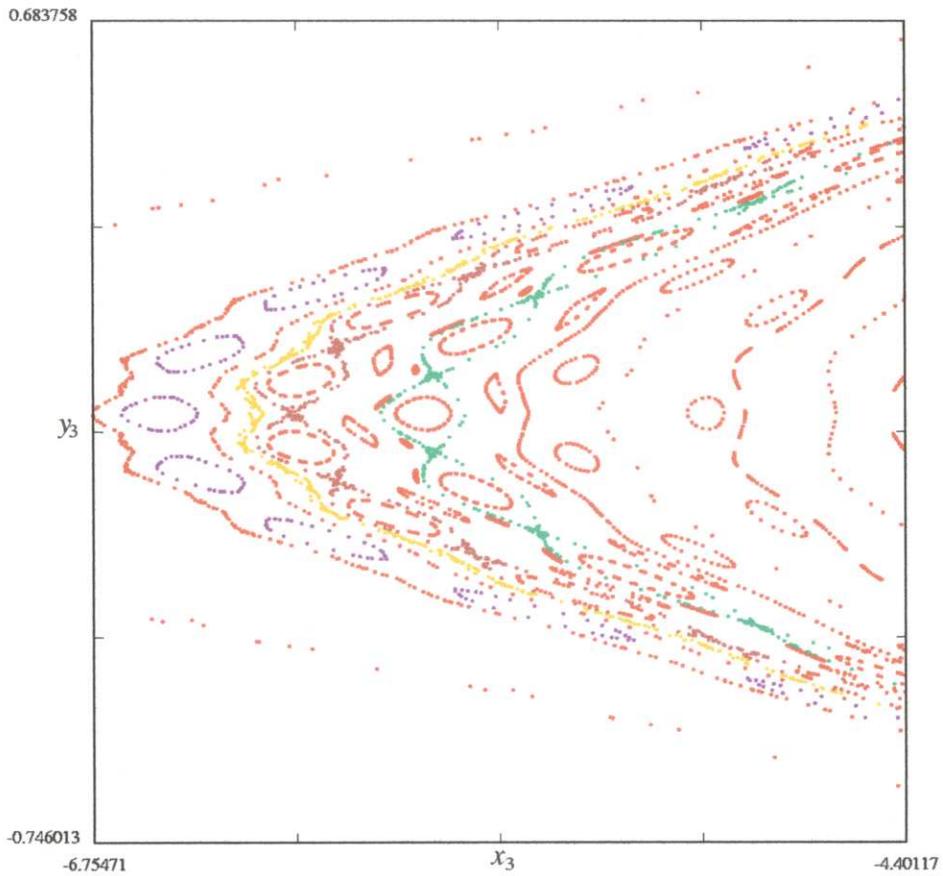

Fig. 12. $A = 0.02$.

Fig. 13. $A = 0.05$.

Fig. 14.   Away from the origin, $A = 0.05$.

exclude a neighborhood of the origin as it is difficult to see any island structure in this region, even for relatively large A-values (see Figs. 9 and 10).

For a small perturbation ($A = 0.01$), most of the P_τ-orbits lie on invariant curves (Fig. 11).

There is only one island clearly evident at this scale (near $(x_3, y_3) = (-3, 0)$). This supports the fact that the measure of the set of P_τ-invariant curves approaches the measure of the set of P-invariant curves as $A \to 0$.
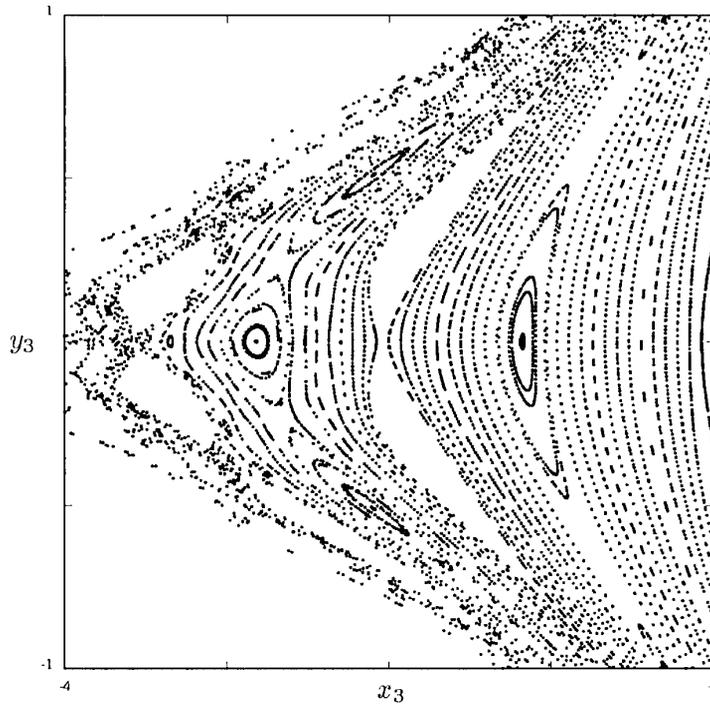

Fig. 15. $A = 0.1$.
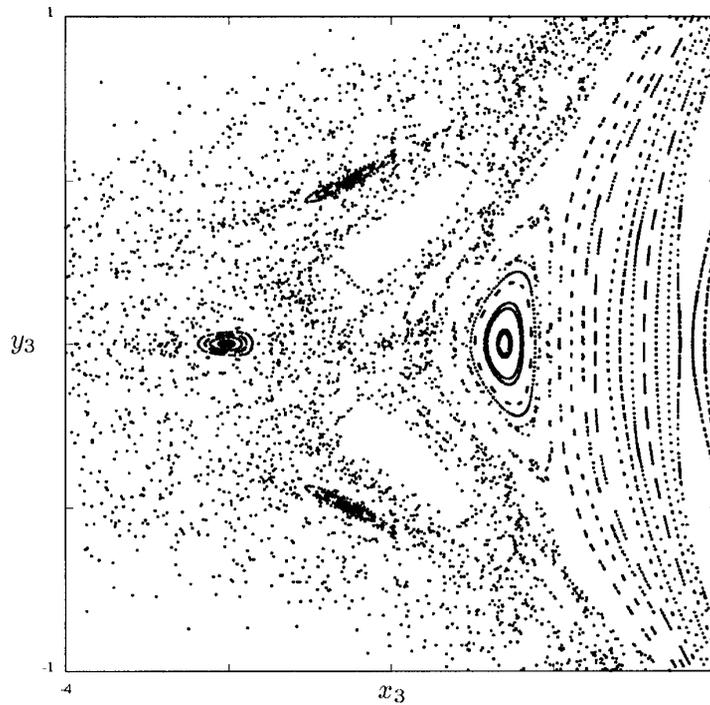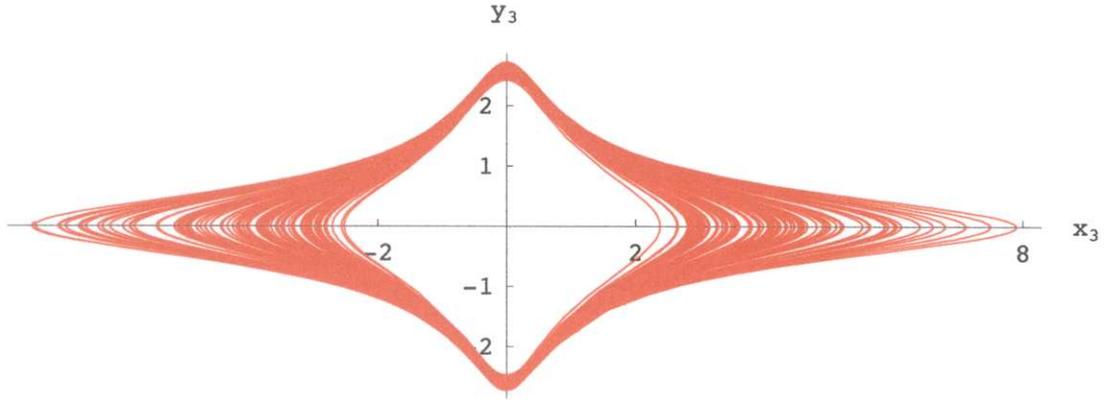

Fig. 16. $A = 0.2$.

Fig. 17.   Small mass trajectory for $A = 0.2$, $(x_3(0), y_3(0)) = (-3.7, 0)$.

As A is increased to 0.02, a second island appears closer to the origin (Fig. 12). Moving along the x_3-axis, a few of the invariant curves are pinching together, indicative of saddle periodic points.

Increasing A to 0.05 yields many fewer invariant curves and the first clear appearance of island chains and saddle periodic points (Fig. 13). In the center of the larger island to the right is a periodic point of period two. Figure 14 presents the increased complexity of P_τ-orbits away from a neighborhood of the origin.

In Figs. 15 and 16, the invariant curves continue to break up and the chaotic behavior resulting from homoclinic tangles becomes more prevalent. The self-similarity of the island chain structure can also be discerned. Figure 17 is the projection onto (x_3, y_3)-space of the solution to system (9) with $A = 0.2$ and initial condition $(x_3(0), y_3(0)) = (-3.7, 0)$.

This sequence of plots clearly illustrates model behavior predicted by the theoretical analysis of our system of equations.

9.   Comments

As the parameter A is increased, the P_τ-phase plane changes dramatically. In particular, the origin passes from an elliptic fixed point to a saddle fixed point (Figs. 18 and 19). The two curves of initial conditions corresponding to $W^s(\mathbf{0})$ yield P_τ-orbits which converge to $(0, 0)$, a surprising result when interpreted in terms of the motion of the small mass. Figure 20 presents the projection of the solution to (9) and the corresponding P_τ-orbit for $A = 0.4$ with initial condition $(x_3(0), y_3(0)) = (0.001, 0)$.

To ascertain the stability type of the fixed point at $(x_3, y_3) = (0, 0)$, the eigenvalues of the matrix $DP_\tau(0, 0)$ must be determined. For Poincaré maps, this corresponds to finding the Floquet multipliers [Hartman, 1982; Perko, 1991; Guckenheimer & Holmes, 1983] which, in theory, are computed as follows. Let $\gamma(s)$ denote the periodic solution to system (11) having initial condition $(x_3(0), y_3(0), t(0)) = (0, 0, 0)$. Recall $\gamma(s)$ is a periodic solution of period τ as we are taking t mod τ.

Let $\mathbf{V}$ be the vector field corresponding to system (11) and let $\mathbf{x} = (x_3, y_3, t)$. To compute the Floquet multipliers, one solves

$$\dot{\mathbf{X}} = (D_{\mathbf{x}}\mathbf{V})(\gamma(s))\mathbf{X}, \quad \mathbf{X}(0) = I_3, \qquad (12)$$

where $\mathbf{X}$ is a 3×3 time-dependent matrix. The Floquet multipliers are the eigenvalues of the matrix $\mathbf{X}(\tau)$. Corresponding to the direction along $\gamma(s)$ is the eigenvalue 1; the remaining two eigenvalues may determine the nature of the fixed point $(x_3, y_3) = (0, 0)$ (complex conjugate eigenvalues need not imply the fixed point is elliptic [Hale & Koçak, 1991]).

In practice, it is difficult to compute Floquet multipliers. In our setting, we must solve (12) with

$$D_{\mathbf{x}}\mathbf{V}(\gamma(s)) = \begin{bmatrix} 0 & 1 & 0 \\ \dfrac{8mx_1(s)^2 - m\varepsilon^2}{2(x_1(s)^2 + \varepsilon^2/4)^{5/2}} & 0 & 0 \\ 0 & 0 & 0 \end{bmatrix},$$

$$(13)$$

with which we had no success. Note, however, that if we take the crude approximation $x_1(s) \equiv x_1(0) = A$,
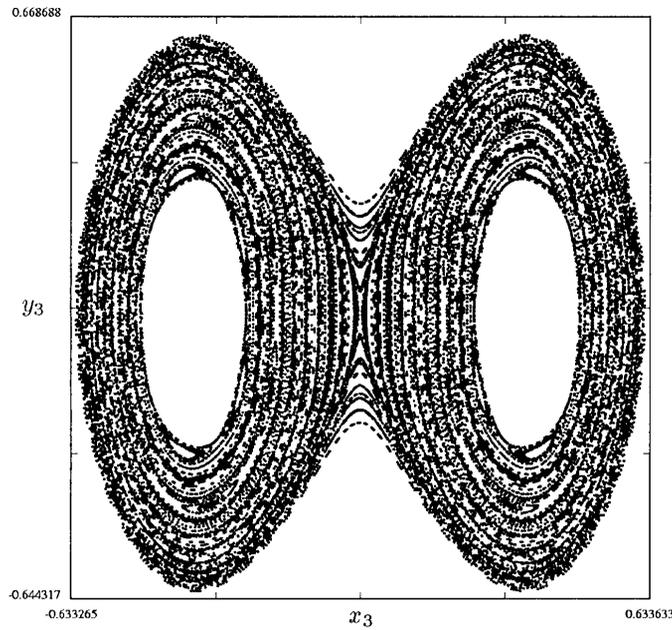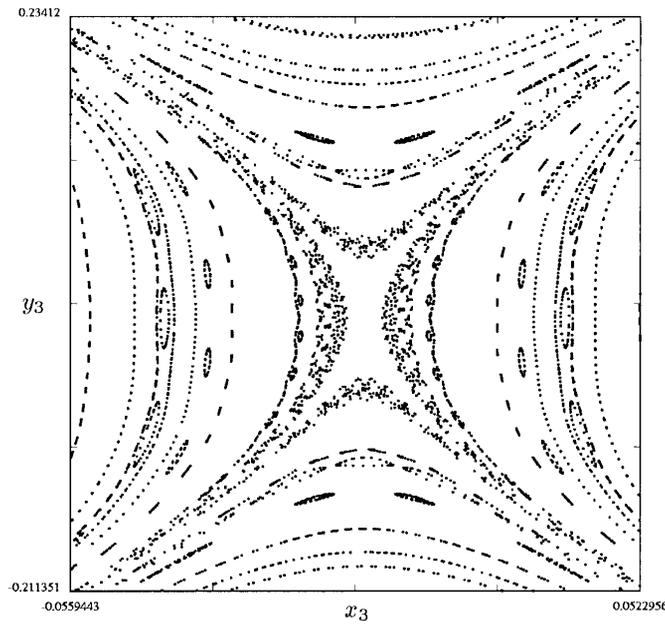
Fig. 18. $A = 0.4$.

Fig. 19. P_τ-phase plane near the origin for $A = 0.4$.

the matrix (13) becomes

$$M = \begin{bmatrix} 0 & 1 & 0 \\ k & 0 & 0 \\ 0 & 0 & 0 \end{bmatrix}, \quad \text{where } k = \frac{8mA^2 - m\varepsilon^2}{2(A^2 + \varepsilon^2/4)^{5/2}}.$$

In this case the solution to (12) is $\mathbf{X}(s) = e^{Ms}$, and the Floquet multipliers are $\zeta_i = e^{\lambda_i \tau}$, where

$\lambda_1 = \sqrt{k}$, $\lambda_2 = -\sqrt{k}$ and $\lambda_3 = 0$. If A is small relative to ε, $k < 0$, and ζ_1 and ζ_2 are a pair of complex conjugate multipliers as expected. If $k > 0$, however, $\zeta_1 > 1$ and $\zeta_2 < 1$, implying $(x_3, y_3) = (0, 0)$ is a saddle. With $\varepsilon = 1$, the constant k changes sign at $A = 1/2\sqrt{2} \approx 0.353$. Via simulations with $\varepsilon = m = 1$, we determined the origin changes from
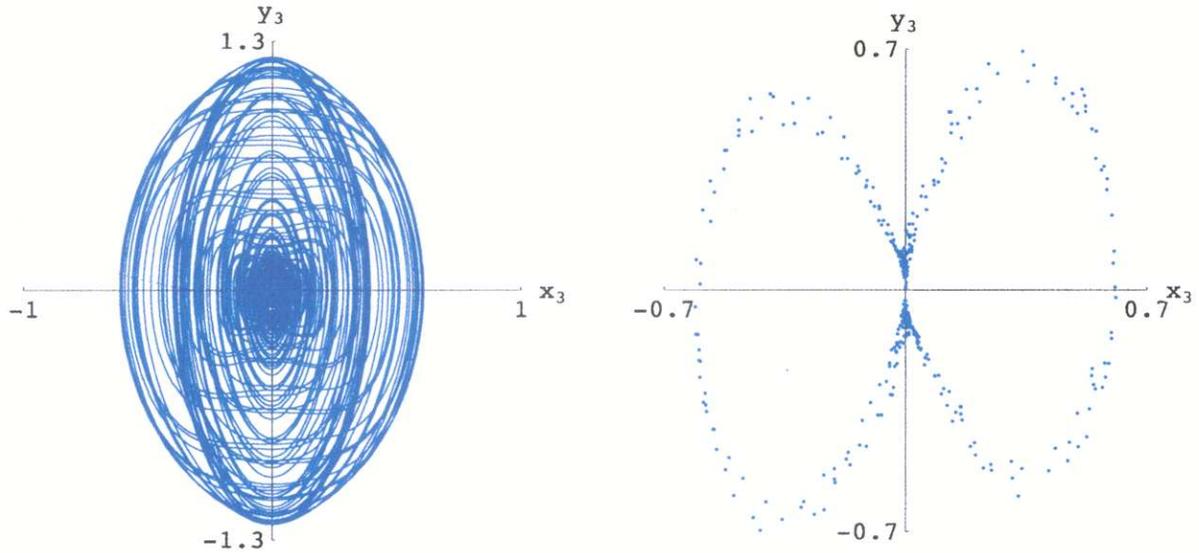
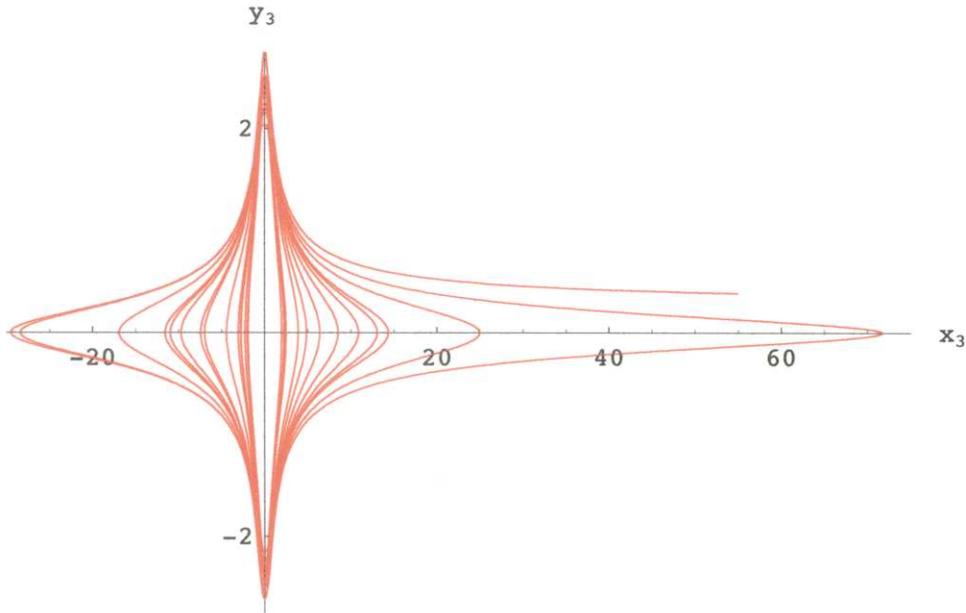Fig. 20.   Small mass trajectory and P_τ-orbit for $A = 0.4$, $(x_3(0), y_3(0)) = (0.001, 0)$.

Fig. 21.   An oscillatory solution?

elliptic to saddle type at $A = 0.308$, a coarse approximation to $1/2\sqrt{2}$.

We were also intrigued by the behavior illustrated in Fig. 21, in which the small mass appears to travel ever-greater distances, always returning to a neighborhood of the origin before setting off again. Let $d(t)$ denote the distance of m_3 from the origin. An *oscillatory solution* is a solution for which $\limsup_{t\to+\infty} d(t) = +\infty$ and $\liminf_{t\to+\infty} d(t) <$

$+\infty$. The existence of oscillatory solutions in the planar restricted three-body problem is proved using symbolic dynamics [Llibre & Simo, 1980]. We are attempting to use symbolic dynamics techniques to gain greater insight into the behavior of our model.

Finally, what happens as $\varepsilon \to 0$? Does an understanding of our model as $\varepsilon \to 0$ yield any insight into the dynamics of the collinear three-body problem?

Acknowledgments

References

Arnol'd, V. I. [1963] "Proof of A. N. Kolmogorov's theorem on the preservation of quasiperiodic motions under small perturbations of the Hamiltonian," *Russ. Math. Surv.* **18**, 9–36.

Arnol'd, V. I. & Avez, A. [1988] *Ergodic Problems of Classical Mechanics* (Addison-Wesley, Redwood City).

Arrowsmith, D. K. & Place, C. M. [1990] *An Introduction to Dynamical Systems* (Cambridge University Press, Cambridge).

Back, A., Guckenheimer, J., Myers, M., Wicklin, F. & Worfolk, P. [1992] "*dstool*: Computer assisted exploration of dynamical systems," *Notices Amer. Math. Soc.* **39**, 303–309.

Barrow-Green, J. [1997] *Poincaré and the Three Body Problem* (American Mathematical Society, Providence).

Guckenheimer, J. & Holmes, P. [1983] *Nonlinear Oscillations, Dynamical Systems, and Bifurcations of Vector Fields* (Springer-Verlag, NY).

Hale, J. & Koçak, H. [1991] *Dynamics and Bifurcations* (Springer-Verlag, NY).

Hartman, P. [1982] *Ordinary Differential Equations*, 2nd edition (Birkhäuser, Boston).

Hénon, M. [1983] "Numerical exploration of Hamiltonian systems," in *Comportement Chaotique des Systèmes Déterministes: Les Houches, Session XXXVI, 1981*, eds. Iooss, G., Helleman, R. H. G & Stora, R. (North Holland, NY), pp. 53–170.

Kaplan, S. [1999] "Symbolic dynamics of the collinear three-body problem," *Cont. Math.* **246**, 143–162.

Katok, A. & Hasselblatt, B. [1995] *Introduction to the Modern Theory of Dynamical Systems* (Cambridge University Press, Cambridge).

Kolmogorov, A. [1957] "General theory of dynamical systems and classical mechanics," *Proc. 1954 Int. Congress Math.* (North Holland, NY), pp. 315–333.

Llibre, J. & Simo, C. [1980] "Oscillatory solutions in the planar restricted three-body problem," *Math. Ann.* **248**, 153–184.

McGehee, R. [1971] "Triple collision in the collinear three body problem," *Inv. Math.* **27**, 191–227.

Meyer, K. & Hall, G. R. [1992] *Introduction to Hamiltonian Dynamical Systems and the N-Body Problem* (Springer-Verlag, NY).

Meyer, K. & Wang, Q. [1995] "The collinear three body problem with negative energy," *J. Diff. Eq.* **119**, 284–309.

Moser, J. [1962] "On invariant curves of area-preserving mappings of an annulus," *Nachr. Akad. Wiss. Gottingen Math. Phys. Kl. II* **6**, 1–20.

Newton, I. [1687] *Philosophae Naturalis Principia Mathematica I–III* (The Royal Society, London). Translated by Andrew Motte, 1729. Revised and edited by Florian Cajori, University of California Press, Berkeley, 1934.

Perko, L. [1991] *Differential Equations and Dynamical Systems* (Springer-Verlag, NY).

Poincaré, H. [1881] "Mémoire sur les courbes définies par une équation différentielle," *J. Mathématiques* **7**, 375–422.

Poincaré, H. [1890] "Sur le problème des trois corps et les équations de la dynamique," *Acta* **13**, 1–270.

Poincaré, H. [1899] *Les Méthodes Nouvelles de la Méchanique Céleste* **III** (Gauthier-Villars, Paris).

Robinson, C. [1994] *Dynamical Systems: Stability, Symbolic Dynamics, and Chaos* (CRC Press, Boca Raton).

Siegel, C. L. & Moser, J. [1971] *Lectures on Celestial Mechanics* (Springer-Verlag, Berlin).

Smale, S. [1965] "Diffeomorphisms with many periodic points," in *Differential and Combinatorial Topology*, ed. Cairns, S. (Princeton University Press, Princeton), pp. 63–80.

Westfall, R. S. [1980] *Never at Rest: A Biography of Isaac Newton* (Cambridge University Press, Cambridge).